
3D Model-based Zero-Shot Pose Estimation Pipeline

Jianqiu Chen
Harbin Institute of
Technology, Shenzhen

Mingshan Sun
SenseTime Research

Tianpeng Bao
SenseTime Research

Zhao Rui
SenseTime Research

Liwei Wu
SenseTime Research

Zhenyu He*
Harbin Institute of
Technology, Shenzhen

Abstract

Most existing learning-based pose estimation methods are typically developed for non-zero-shot scenarios, where they can only estimate the poses of objects present in the training dataset. This setting restricts their applicability to unseen objects in the training phase. In this paper, we introduce a fully zero-shot pose estimation pipeline that leverages the 3D models of objects as clues. Specifically, we design a two-step pipeline consisting of 3D model-based zero-shot instance segmentation and a zero-shot pose estimator. For the first step, there is a novel way to perform zero-shot instance segmentation based on the 3D models instead of text descriptions, which can handle complex properties of unseen objects. For the second step, we utilize a hierarchical geometric structure matching mechanism to perform zero-shot pose estimation which is 10 times faster than the current render-based method. Extensive experimental results on the seven core datasets on the BOP challenge show that the proposed method outperforms the zero-shot state-of-the-art method with higher speed and lower computation cost.

1 Introduction

Pose estimation plays a crucial role in various robotic and augmented reality applications. Existing deep-learning methods [1–3] achieve remarkable performance for seen objects after absorbing a large amount of training data for each target object. However, when there is a novel (unseen) object introduced, it requires significant time and effort to synthesize or annotate data and re-train the model from scratch. This greatly restricts the universality and reusability of models, and the high time and training costs further hinder the practical application of pose estimation with novel objects. Hence, there is a pressing need for a zero-shot pose estimation method that enables training once and generalizing to any unseen object during inference, addressing these challenges effectively.

Upon revisiting pose estimation methods, it is evident that they typically involve two steps. Firstly, an instance segmentation or object detection method is employed to locate and classify the object. Subsequently, a pose estimator is utilized to estimate the pose transformation parameters, which consist of three degrees for rotation and three degrees for translation, from the target object’s coordinate system to the camera coordinate system. However, in the zero-shot setting, where the specific 3D object is unseen and lacks any prior information during the training phase, segmenting and classifying it becomes extremely challenging. Consequently, recent zero-shot pose estimators resort to utilizing supervised non-zero-shot segmentation results to estimate the 6D pose and focus solely on the second step.

*Corresponding author.

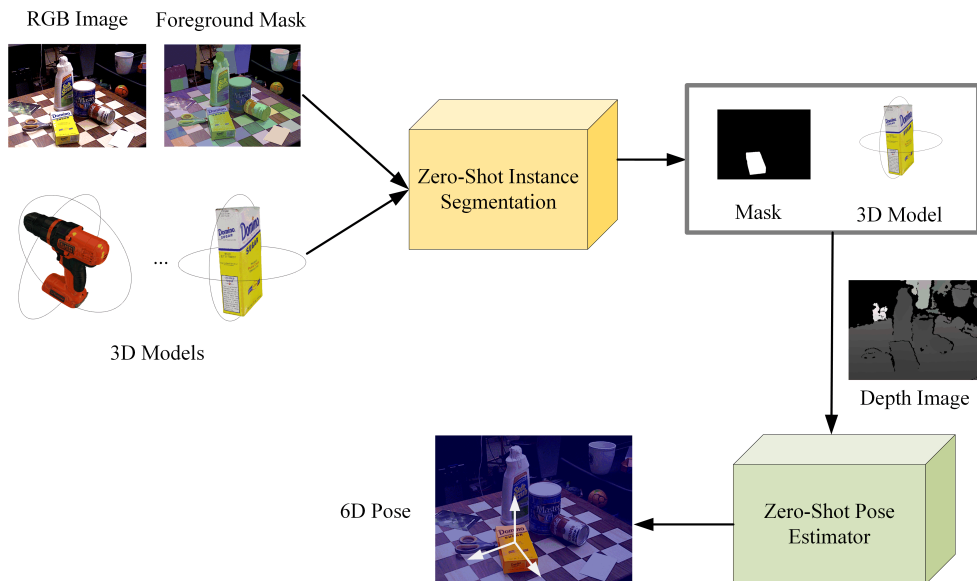


Figure 1: The proposed pipeline for zero-shot pose estimation based on 3D models.

In the first step, most existing zero-shot instance segmentation methods, such as SAM [4], are primarily designed to predict foreground instances or instances associated with specific textual prompts. However, these methods encounter limitations in missing the capabilities of distinguishing the class label (related 3D model) of the candidate instances. In the case of foreground instance segmentation, the method fails to attribute the foreground instance to a specific object without human interaction. In the case of text-prompt instances segmentation, challenges arise in accurately describing complex properties of objects, such as their shape and materials, using natural language. This task requires domain experts with relevant knowledge, especially in specialized fields like industrial manufacturing or robotics applications. Additionally, foundation models may struggle to comprehend these professional descriptions, resulting in difficulties or errors. In summary, the field lacks a dedicated zero-shot instance segmentation method that effectively leverages 3D models.

In the second step, current zero-shot pose estimators, such as MegaPose [5] and Zephyr [6], typically employ an online rendering approach to compare the scene image with rendered images corresponding to candidate pose hypotheses. Although this approach is suitable for the zero-shot scenario, it has a limitation in terms of runtime. The online rendering module requires approximately 2.5 seconds to render each object, leading to a total rendering time of potentially more than ten seconds per image when multiple objects are present.

This paper presents the pioneering work on a fully zero-shot pose estimation pipeline, as illustrated in Fig 1. Specifically, we have designed a two-step pipeline that incorporates 3D model-based zero-shot instance segmentation and zero-shot pose estimator. In the instance segmentation step, we introduce the utilization of 3D models to render and extract multi-view clues, enabling the search for correspondence between the instance from the scene image and candidate target objects. We refer to this approach as "3D model-based zero-shot instance segmentation". In the 6D pose parameter estimating step, we have proposed a zero-shot pose estimator which leverages a hierarchical geometric feature matching module that estimates the best pose parameters by minimizing the matching point pairs' distance from the target object coordinates to the camera coordinates. Compared with the online rendering mechanism in current SOTA zero-shot methods, the hierarchical geometric feature matching module shows a significant advantage in efficiency. It requires only 0.2 seconds for each object, making it 10 times faster than the current state-of-the-art method [5].

In summary, our paper makes the following key contributions:

- Introduction of a fully zero-shot pose estimation pipeline.
- Proposal of a novel 3D model-based zero-shot instance segmentation method.
- Development of a zero-shot pose estimator based on hierarchical geometric feature matching.
- Extensive experimental results demonstrate that our proposed method outperforms the zero-shot state-of-the-art method while offering higher speed and lower computation cost.

2 Related Work

In this section, we will begin by providing an overview of the existing research on the zero-shot instance segmentation problem. Subsequently, we will delve into the extensive research conducted on the zero-shot 6D pose estimation.

2.1 Zero-Shot Instance Segmentation

Instance segmentation involves predicting a mask for each object and assigning corresponding class labels. It is typically performed as a prerequisite task for 6D pose estimation. However, previous research [7–9, 4, 10] has primarily concentrated on zero-shot semantic segmentation and zero-shot category-agnostic instance segmentation. UOIS-Net [7] separately leverages synthetic RGB and synthetic depth for unseen object instance segmentation. Subsequently, Xiang et al. [8] utilized a metric learning loss function to produce pixel-wise feature embeddings such that pixels from the same object are close to each other and pixels from different objects are separated in the embedding space. With the learned feature embeddings, a mean shift clustering algorithm can be applied to discover and segment unseen objects. These two methods assign different labels to different objects, but they fail to identify multiple objects of the same category as belonging to the same class. SuperRGB-D [9] explore zero-shot instance segmentation from RGB-D data to identify unseen objects in a semantic category-agnostic manner. Inspired by the development of prompt-based universal interfaces for large language models, both SAM [4] and SEEM [10] propose a model that is purposefully designed and trained to be promptable. This promptable model exhibits the ability to effectively transfer its knowledge and skills in a zero-shot manner to novel image distributions and tasks. However, the aforementioned methods do not perform instance segmentation for each individual instance based on its own category. To enhance the accuracy of our approach in labeling different segmented instances, we leverage 3D model-rendered images to identify the most similar instance. By utilizing the more detailed features provided by the rendered images, our method improves the precision of instance selection compared to relying solely on textual descriptions.

2.2 Zero-Shot 6D Pose Estimation

Zero-shot 6D pose estimation is the task of determining the 6D pose of novel objects that have not been included in the training data. In other words, this involves estimating the pose of objects that were not seen or encountered during the model training phase. The first attempts to tackle this problem involved establishing correspondences using locally invariant features [11–15]. By using oriented point pair features, PPF [15] generates a global model description and employs a fast voting scheme to perform local matching of the model. Convolutional neural networks (CNNs) [6, 5] have replaced the previously used methods, such as those based on hand-crafted features, for 6D pose estimation. The current trend is to use learning-based approaches that utilize CNNs to achieve higher accuracy and robustness. Zephyr [6] uses a hypothesis generation and scoring framework that focuses on training a scoring function capable of generalizing to novel objects. To achieve zero-shot generalization, it rates hypotheses based on differences between unordered points. MegaPose [5] introduces a 6D pose refinement method that employs a render-and-compare strategy, capable of handling novel objects. To enable the network to process unknown objects, MegaPose provides shape and coordinate system information as inputs, achieved by online rendering multiple synthetic views of the object’s 3D model. Deep learning methods for 6D pose estimation rely on 3D model rendering from multiple views, which can result in incomplete capture of the object’s 3D structure. Moreover, multiple rendered images are required as input for each instance in a scene, leading to increased computational costs. To preserve the local 3D structural information, our method avoids the use of online rendered images and instead inputs corresponding 3D models and scene point clouds directly.

They are then locally matched by a hierarchical geometric feature-matching mechanism. The 6D pose parameters for each instance in the scene can be obtained from a single input by minimizing the transformation distance.

3 Method

Fig 2 illustrates our detailed implementation of the proposed zero-shot pose estimation pipeline which consists of two steps. We will provide a thorough explanation of the two steps in the following subsections, respectively.

3.1 3D Model-based Zero-Shot Instance Segmentation

As indicated by the yellow box in Fig 2, the target of the instance segmentation step is to search all potential instances related to the provided 3D models. To leverage the 3D model clues, we offline render the 3D model from different camera views achieving a set of 2D template images. A visual foundation model ImageBind [16] is utilized to extract visual features from the template images as the visual clues of the 3D model, which can be presented in F_t with shape (N, R, C) , where N is the number of target objects, R is the number rendered template images and C is the feature dimension for visual foundation model.

For the scene image, we adopt an interactive segmentation method SAM [4] taking a uniform point set as a prompt to generate all foreground masks without labels. Then, similar to the template images, we crop all foreground instances and extract their visual features through the same visual foundation model as the template images. It presents as F_s with shape (M, C) where M is the number of foreground masks. To filter the potential instances from all foreground instances, a feature similarity filter module is introduced. It calculates the cosine feature similarity between scene instances F_s and template objects F_t :

$$\mathbf{C} = \left(\frac{\mathbf{F}_s}{\|\mathbf{F}_s\|} \right) \left(\frac{\mathbf{F}_t}{\|\mathbf{F}_t\|} \right)^T, \quad (1)$$

where the matrix C is with shape (M, N, R) and any element in it is the cosine distance with the range $(-1, 1)$. The higher cosine distances mean higher feature similarities.

We select the max feature similarity for all render template images as the corresponding target object’s predicted score. The scene instance whose prediction score is larger than the threshold is viewed as a candidate instance, the corresponding target object selects the highest score if there is more than one higher than the threshold.

3.2 3D Model-based Zero-Shot Pose Estimator

As indicated by the green box in Fig 2, the target of the pose estimator is to estimate the target object’s rigid transformation \mathbf{R}, \mathbf{t} from the target object’s object coordinate systems to the camera coordinate system, where $\mathbf{R} \in SO(3)$ is a 3D rotation and $\mathbf{t} \in \mathbb{R}^3$ is a 3D translation. To effectively and efficiently estimate the pose transformation, we choose the point cloud feature as input and leverage a hierarchical geometric feature matching module to estimate the pose parameter when transforming the object point cloud from the object coordinate systems to the camera coordinate systems. However, it is challenging to establish point correspondences between two point clouds acquired through different methods (3D scan vs. consumer-grade depth sensors) due to variations in density and visibility. For the 3D Model, a set of point clouds $\mathcal{O} = \{\mathbf{o}_i \in \mathbb{R}^3 \mid i = 1, \dots, n\}$ is uniformly sampled from the surface of the mesh. For the scene points, the mask is applied to index the object region from the depth image and convert it into a scene point cloud $\mathcal{S} = \{\mathbf{s}_i \in \mathbb{R}^3 \mid i = 1, \dots, m\}$. The scene point cloud refers to a subset of the 3D model point cloud that contains only the visible region that can be captured. Different viewpoints of the camera will correspond to a specific visible region in the object 3D model. Besides, the scene point cloud is captured from the depth sensor and cropped from the detection mask, which unavoidably includes some surrounding noisy points. Unfortunately, most point cloud’s down sample methods such as Farthest Point Sampling (FPS) or grid sampling are prone to keep the noisy points due to the sampling mechanism. Therefore, due to the mismatched

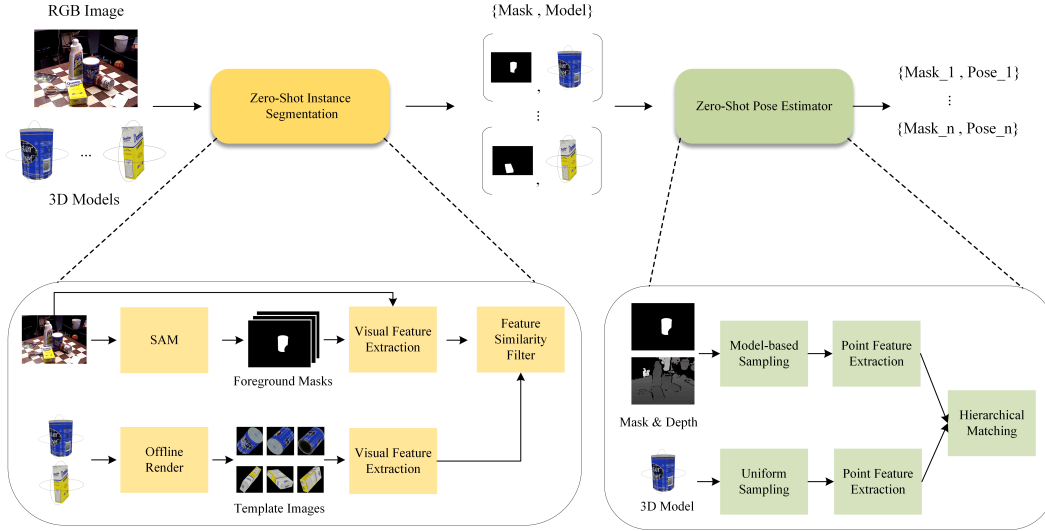


Figure 2: Overview architecture of 3D model-based zero-shot instance segmentation and pose estimator. The first step involves segmenting all candidate instances and classifying their corresponding 3D models using the RGB image as input. The second step leverages the depth image and the predicted mask to generate the scene point cloud and estimates the pose parameter based on the hierarchical geometric feature matching.

receptive fields, it interferes with the calculation of point cloud correspondence \mathcal{C} , thereby decreasing the performance in fitting the best pose parameters by minimizing the following equation.

$$\min_{\mathbf{R}, \mathbf{t}} \sum_{(\mathbf{o}_{x_i}, \mathbf{s}_{y_i}) \in \mathcal{C}} \|\mathbf{R} \cdot \mathbf{o}_{x_i} + \mathbf{t} - \mathbf{s}_{y_i}\|_2^2, \quad (2)$$

where \mathbf{s}_{y_i} and \mathbf{o}_{x_i} are matched corresponding points.

To alleviate this problem, we introduce a simple but effective 3D model-prior-based sampling method that holds the comparable feature receptive fields. We adopt the object circumradius as a prior constraint to cluster the scene point through a Mean-Shift algorithm with the bandwidth of the object circumradius, which controls the proximity range between scene and object point clouds by adjusting the clustering bandwidth. Taken the cluster with the highest number of the points as the foreground points. When holding the comparable feature receptive fields, we can leverage hierarchical features on both scene and object point clouds to match each other.

We follow GeoTransformer[17] to extract hierarchical point cloud features. As shown in Fig 3, the high-level feature with a larger receptive field (the red boxes) can be seen as a set of viewpoints from the 3D Model to locate the visible region. After that, a low-level feature is applied to find the point-to-point correspondence (green dotted lines) between the predicted visible region of the target object and the scene point cloud. The hierarchical design limits the matching scope in the visible area and alleviates the mismatching between visible and invisible regions. Based on the correspondence, we minimize the point cloud distance in Eq 2 to calculate a target R, t through Singular Value Decomposition (SVD).

We train the model on the large-scale 3D model dataset GSO [18] to learn viewpoint matching and local geometric structure matching. First, we leverage the features from the visible region of the 3D model and its corresponding scene point cloud area as positive samples. The others that have an overlap of less than a threshold are viewed as negative samples. Since the visible region may contain more than one feature point with comparable overlaps, we adopt the overlap-aware circle loss [17] to

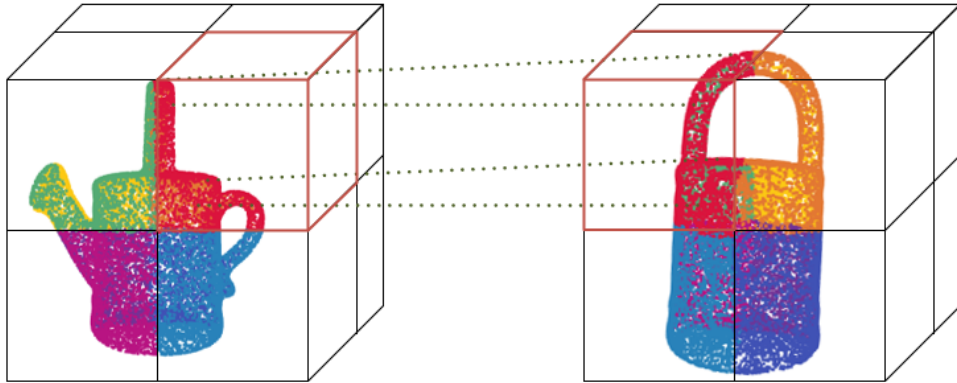


Figure 3: Hierarchical matching mechanism in the zero-shot pose estimator. A hierarchical geometric feature matching that higher level feature to locate the potentially visible region (red boxes) and predict the point correspondences ((green dotted lines) in this region by local structure feature similarity.

train the model to focus on the high overlap feature points matching. For local geometric structures, the low-level scene points are matched with 3D model points transformed by ground truth pose with a matching radius. The predicted correspondence matrix is calculated from the cosine similarity of features with an extra learnable mismatch dustbin feature to indicate the noisy points and invisible points. The negative log-likelihood loss is applied to fit the matching correspondence.

4 Experiments

4.1 Benchmark Datasets

For the training dataset, we take the GSO [19] to train our pose estimation module, which contains 1000 3D objects under household scenes and 1 million synthetic images provided by Megapose [5]. For the test datasets, we evaluated our method on the seven core datasets of the BOP challenge [20], including LineMod Occlusion (LMO), T-LESS, TUD-L, IC-BIN, ITODD, HomebrewedDB (HB) and YCB-Video (YCB-V). These datasets are enriched with diverse factors of variation, including texture, symmetry, and household or industrial scenes, which accurately represent the different types of objects typically encountered in daily and robotic scenarios.

4.2 Instance Segmentation Metric

We evaluate the performance of instance segmentation by Average Precision (AP) and Average Recall (AR) following the COCO metric and the BOP Challenge. The metric of the AP is the mean of AP at different Intersection over Union (IoU=.50:.05:.95) values. AR is the maximum recall achieved when a fixed number (100 for the demonstration) of detections per image is considered.

4.3 Pose Estimation Metrics

In measuring the accuracy of an estimated pose \hat{P} in relation to the ground-truth pose \bar{P} of an object model M , we utilize the mean Average Recall of three pose-error functions, calculated by $AR = (AR_{VSD} + AR_{MSSD} + AR_{MSPD})/3$ and more information about evaluation metrics for the threshold to calculate the AR can be obtained from the competition [20]. Here is a brief distribution for each part of the metric.

4.3.1 VSD (Visible Surface Discrepancy)

VSD deems poses that possess an equal shape to be identical as it only assesses the error in the object’s visible section.

$$e_{VSD}(\hat{D}, \bar{D}, \hat{V}, \bar{V}, \tau) = \text{avg}_{p \in \hat{V} \cup \bar{V}} \begin{cases} 0 & \text{if } p \in \hat{V} \cap \bar{V} \wedge |\hat{D}(p) - \bar{D}(p)| < \tau \\ 1 & \text{otherwise} \end{cases} \quad (3)$$

To calculate the distance maps \hat{D} and \bar{D} , it renders the 3D model M in the predicted pose \hat{P} and ground truth pose \bar{P} , respectively. \hat{V} and \bar{V} are visibility masks, which are obtained by comparing them with the distance maps of the test image. The τ is the tolerance parameter.

4.3.2 MSSD (Maximum Symmetry-Aware Surface Distance)

The set S_M contains global symmetry transformations of the 3D model, and V_M represents a set of vertices of the model. The maximum distance among the vertices of the model plays a crucial role in robotic manipulation. In this context, a larger maximum surface deviation suggests a higher probability of a successful grasp.

$$e_{MSSD}(\hat{P}, \bar{P}, S_M, V_M) = \min_{S \in S_M} \max_{X \in V_M} \|\hat{P}x - \bar{P}Sx\|_2 \quad (4)$$

4.3.3 MSPD (Maximum Symmetry-Aware Projection Distance)

The function `proj` represents the pixel-level 2D projection, while the other variables have the same meaning as in MSSD. MSPD takes into account the global object symmetry and replaces the mean with the maximum distance to enhance the robustness of the object model’s geometry and sampling.

$$e_{MSPD}(\hat{P}, \bar{P}, S_M, V_M) = \min_{S \in S_M} \max_{X \in V_M} \|\text{proj}(\hat{P}x) - \text{proj}(\bar{P}Sx)\|_2 \quad (5)$$

4.4 Evaluation of Zero-Shot Instance Segmentation

We conduct the experiments on seven BOP Challenge datasets and use the Average Precision (AP) as the metric to evaluate the proposed method. Since there are no other related methods following the 3D Model-Based Zero-Shot Instance Segmentation setting, we select two supervised non-zero-shot methods and implement a text-based zero-shot instance segmentation method for comparison. The Mask RCNN method [21] is from the CosyPose [22], which is trained on the real or synthetic training datasets for each test object. The ZebraPoseSAT [23] is the current SOTA method for the instance segmentation task, which leverages a two-stage setting that detection for coarse locating and pose estimation network for refinement. For the text-based zero-shot instance segmentation, we hold the same pipeline with our method and adopt the class name as a text feature, instead of the template image features to evaluate and compare the performance. For the T-LESS, TUD-L, and HB datasets, there are only object IDs without class names provided. As depicted in Tab 1, our 3D model-based zero-shot instance segmentation method shows obvious performance improvements compared with the text-based method from 6.7 % to 21.4 %. However, there is still a performance gap compared with the supervised methods.

4.5 Evaluation of Zero-Shot Pose Estimation

To evaluate our pose estimation performance, we compared the supervised methods without zero-shot setting and the latest zero-shot pose estimation methods. The zero-shot task can not achieve any object prior which is quite challenging and has performance limitations compared with the supervised

Table 1: Evaluation of zero-shot instance segmentation results on the seven core datasets in the BOP challenge. The metric is the Average Precision (AP) at different Intersection over Union (IoU=.50:.05:.95) values. * denotes that there is no object name provided and inferred by the object id. Real denotes the use of real annotation data for training.

Method	Zero-Shot	Real	LM-O	T-LESS	TUD-L	IC-BIN	ITODD	HB	YCB-V	Mean
Mask RCNN[21]	✗	✗	37.5	51.7	30.6	31.6	12.2	47.1	42.9	36.2
Mask RCNN[21]	✗	✓	37.5	54.4	48.9	31.6	12.2	47.1	42.9	39.2
ZebraPoseSAT[23]	✗	✗	50.6	62.9	51.4	37.9	36.1	64.6	62.2	52.2
ZebraPoseSAT[23]	✗	✓	50.6	70.9	70.7	37.9	36.1	64.6	74.0	57.8
Text-based	✓	✗	6.5	0.0*	0.0*	9.8	3.6	0.0*	27.3	6.7
Ours	✓	✗	17.6	9.6	24.1	18.7	6.3	31.4	41.9	21.4

Table 2: Evaluation of zero-shot pose estimation results on the BOP dataset. The metric is the Average Recall (AR) in BOP Challenge [20]. Note that our method is based on the proposed zero-shot instance segmentation method while the other methods including MegaPose are based on non-zero-shot object detectors or segmentors.

Method	Zero-Shot	LM-O	T-LESS	TUD-L	IC-BIN	ITODD	HB	YCB-V	Mean
DPOD[24]	✗	16.9	8.1	24.2	13.0	0.0	28.6	22.2	16.1
CosyPose[22]	✗	53.6	52.0	57.6	53.0	13.1	33.5	33.3	42.3
EPOS[25]	✗	54.7	46.7	55.8	36.3	18.6	58.0	49.9	45.7
MegaPose[5]	✓	18.7	19.7	20.5	15.3	8.00	18.6	13.9	16.4
Ours	✓	14.2	6.3	24.9	18.7	13.6	23.6	22.9	17.7

method. Compared with the zero-shot method Megapose [5], our method achieves 1.3% performance gain with ten times speed and our method does not require any online image rendering which is the crux when porting to real applications due to heavy computation cost. Besides, the megapose [5] has a limitation in that it is required a supervised Mask RCNN to locate the candidate object but our method is able to estimate the pose in and fully zero-shot pipeline with a comparable performance.

4.6 Time Efficiency

Compared to current zero-shot 6D pose estimation methods, the proposed pose estimation method based on point cloud matching eliminates the time-consuming online image rendering operation. As presented in Table 3, our method achieves an impressive pose estimation time of 0.2 seconds per object, which is ten times faster than the current state-of-the-art zero-shot method[5].

In terms of the instance segmentation step, since the rendering of templates is conducted offline, the zero-shot instance segmentation requires only 0.8 seconds per image. Consequently, the overall pipeline demonstrates higher efficiency compared to current methods, enabling its application in various downstream tasks without the limitations imposed by time constraints.

4.7 Ablation Study

4.7.1 Comparison of the Number of Template Images

To investigate the effect of the number of rendered template images for each 3D model of the target object, we select four settings for 6, 72, 512, and 576. For 6 template images, it uses the front, back, left, right, up, and down direction of the object to render template images. The others are sampled from a uniform sequence over SO(3) sphere with different densities following [26]. As shown in 4, we demonstrate the GPU memory consumption, inference running time, and accuracy for different rendered template images of each target object’s 3D model. The sparse rendered template images have the worst robustness for visual ambiguity when objects have a similar appearance though there is a minor advantage in the speed and memory consumption. For rendering template images from

Table 3: Time efficiency for zero-shot pose estimation on the YCB-V dataset.

Method	Runtime per object (s)
Megapose[5]	2.5
Ours	0.2

Table 4: Comparison of the number of template images for each object on the YCB-V dataset.

Number	Memory (MB)	Time (s)	AP (%)	AR (%)
6	0.023	0.33	39.4	48.8
72	0.281	0.33	41.9	53.1
512	2.000	0.34	41.3	56.4
576	2.250	0.34	40.5	55.9

Table 5: Comparison of the 3D model-based sampling mechanism for pose estimation AR metric.

Sampling	LMO(AR %)	YCB-V(AR %)
Without	13.4	22.8
With	14.2	27.3

Table 6: Comparison of different visual foundation models on the YCB-V dataset, with the evaluation metrics of AP and AR for instance segmentation.

Visual Model	AP (%)	AR (%)
SLIP[27]	13.2	28.7
ImageBind[16]	41.6	53.1

uniform $SO(3)$ space, the rendered image appearance gap between observation and template rendered views is reduced which shows improvement in accuracy. However, when the density of rendered template images increases to 512 and 576, the AP slightly decreases, and the AR increases. This shows that our methods are not required a large number of rendered template images. To balance efficiency and effectiveness, we choose the 72 in our method for all test datasets.

4.7.2 Comparison of The 3D Model-based Sampling Mechanism

To validate the effectiveness of the proposed sampling mechanism at the local structure matching module, we compare the pose estimation performance with and without this mechanism. As demonstrated in Tab 5, this sampling mechanism is able to improve the matching accuracy and shows 0.8% improvement.

4.7.3 Comparison of Different Visual Foundation Models

The visual feature extraction foundation models depend on the accuracy and robustness of the label selection in the zero-shot instance segmentation step. There is an experiment for two different foundation modules SLIP [27] (an advanced version of CLIP [28]) and ImageBind [16] (a recent multi-modal pertaining method). The results in Tab 6 show that a larger and stronger foundation model increases the average precision and recall significantly.

4.8 Implementation Details

The zero-shot pose estimation pipeline is trained on the cluster with 8 NVIDIA V100 and inferring on the PC with NVIDIA RTX 3090.

Foreground Instance Segmentation It adopts the recent SOTA interactive segmentation method [4], uniform set 16 per image as the prompt of Decoder to generate the foreground instances’ masks and filtering the noisy region where the mask area is small than 200 pixels.

Visual Feature Extraction The large-scaled visual foundation model ImageBind [16] takes the resized image with (224, 224, 3) shape as input to extract the scene images and template images visual features in (N, C) where N is the number of images and C is the feature dimension for 1024 in this experiment.

Feature Similarity Filter We adopt the cosine similarity as a metric to filter the instances which are not related to our 3D models. For each candidate object, the max feature similarity for all template views to the scene instance is chosen. When feature similarities between scene instances and template images are larger than the threshold, these scene instance is the candidate and the related object is selected by the highest feature similarity between the candidate image and template images.

Hierarchical Matching Mechanism We keep the similar network architecture in [17] that leverages the KPConv [29] as the backbone to extract hierarchical point cloud features and matches the

potentially visible regions based on the feature from level 4 and points matching based on the feature from level 2.

5 Conclusion

In this paper, we propose a fully zero-shot pose estimation pipeline based on the 3D model. Our pipeline consists of a 3D model-based zero-shot instance segmentation module to segment the candidate object from the scene image and a zero-shot pose estimator is introduced to estimate the pose transformation between the object coordinate system to the camera coordinate system based on the hierarchical point cloud structure matching mechanism. The proposed method outperforms the zero-shot state-of-the-art method but with higher speed and lower computation cost. There is a limitation in that 3D models are not used as prompts in the zero-shot instance segmentation module because SAM [4] only supports text, point, box, and mask prompts. We will try to explore a multi-modality model to support 3D model prompts in future work. The proposed pipeline operates fully in a zero-shot setting and demonstrates faster performance compared to previous approaches. This pipeline holds promise for inspiring innovative solutions in various fields, including industrial manufacturing, robotics, and beyond.

References

- [1] Yisheng He, Wei Sun, Haibin Huang, Jianran Liu, Haoqiang Fan, and Jian Sun. Pvn3d: A deep point-wise 3d keypoints voting network for 6dof pose estimation. In *Proceedings of the IEEE/CVF conference on computer vision and pattern recognition*, pages 11632–11641, 2020.
- [2] Yisheng He, Haibin Huang, Haoqiang Fan, Qifeng Chen, and Jian Sun. Ffb6d: A full flow bidirectional fusion network for 6d pose estimation. In *Proceedings of the IEEE/CVF Conference on Computer Vision and Pattern Recognition*, pages 3003–3013, 2021.
- [3] Mingshan Sun, Ye Zheng, Tianpeng Bao, Jianqiu Chen, Guoqiang Jin, Rui Zhao, Liwei Wu, and Xiaoke Jiang. Uni6dv2: Noise elimination for 6d pose estimation. *arXiv preprint arXiv:2208.06416*, 2022.
- [4] Alexander Kirillov, Eric Mintun, Nikhila Ravi, Hanzi Mao, Chloe Rolland, Laura Gustafson, Tete Xiao, Spencer Whitehead, Alexander C Berg, Wan-Yen Lo, et al. Segment anything. *arXiv preprint arXiv:2304.02643*, 2023.
- [5] Yann Labbé, Lucas Manuelli, Arsalan Mousavian, Stephen Tyree, Stan Birchfield, Jonathan Tremblay, Justin Carpentier, Mathieu Aubry, Dieter Fox, and Josef Sivic. MegaPose: 6D Pose Estimation of Novel Objects via Render & Compare. In *CoRL*, 2022.
- [6] Brian Okorn, Qiao Gu, Martial Hebert, and David Held. Zephyr: Zero-shot pose hypothesis rating. In *2021 IEEE International Conference on Robotics and Automation (ICRA)*, pages 14141–14148. IEEE, 2021.
- [7] Christopher Xie, Yu Xiang, Arsalan Mousavian, and Dieter Fox. Unseen object instance segmentation for robotic environments. *IEEE Transactions on Robotics*, 37(5):1343–1359, 2021.
- [8] Yu Xiang, Christopher Xie, Arsalan Mousavian, and Dieter Fox. Learning rgb-d feature embeddings for unseen object instance segmentation. In *Conference on Robot Learning*, pages 461–470. PMLR, 2021.
- [9] Evin Pınar Örnek, Aravindhana K Krishnan, Shreekanth Gayaka, Cheng-Hao Kuo, Arnie Sen, Nassir Navab, and Federico Tombari. Supergb-d: Zero-shot instance segmentation in cluttered indoor environments. *IEEE Robotics and Automation Letters*, 2023.
- [10] Xueyan Zou, Jianwei Yang, Hao Zhang, Feng Li, Linjie Li, Jianfeng Gao, and Yong Jae Lee. Segment everything everywhere all at once. *arXiv preprint arXiv:2304.06718*, 2023.
- [11] David G Lowe. Object recognition from local scale-invariant features. In *Proceedings of the seventh IEEE international conference on computer vision*, volume 2, pages 1150–1157. Ieee, 1999.
- [12] Herbert Bay, Tinne Tuytelaars, and Luc Van Gool. Surf: Speeded up robust features. *Lecture notes in computer science*, 3951:404–417, 2006.
- [13] Alvaro Collet and Siddhartha S Srinivasa. Efficient multi-view object recognition and full pose estimation. In *2010 IEEE International Conference on Robotics and Automation*, pages 2050–2055. IEEE, 2010.

- [14] Alvaro Collet, Manuel Martinez, and Siddhartha S Srinivasa. The moped framework: Object recognition and pose estimation for manipulation. *The international journal of robotics research*, 30(10):1284–1306, 2011.
- [15] Bertram Drost, Markus Ulrich, Nassir Navab, and Slobodan Ilic. Model globally, match locally: Efficient and robust 3d object recognition. In *2010 IEEE computer society conference on computer vision and pattern recognition*, pages 998–1005. Ieee, 2010.
- [16] Rohit Girdhar, Alaaeldin El-Nouby, Zhuang Liu, Mannat Singh, Kalyan Vasudev Alwala, Armand Joulin, and Ishan Misra. Imagebind: One embedding space to bind them all. In *Proceedings of the IEEE/CVF Conference on Computer Vision and Pattern Recognition*, pages 15180–15190, 2023.
- [17] Zheng Qin, Hao Yu, Changjian Wang, Yulan Guo, Yuxing Peng, Slobodan Ilic, Dewen Hu, and Kai Xu. Geotransformer: Fast and robust point cloud registration with geometric transformer. *IEEE Transactions on Pattern Analysis and Machine Intelligence*, 2023.
- [18] Laura Downs, Anthony Francis, Nate Koenig, Brandon Kinman, Ryan Hickman, Krista Reymann, Thomas B McHugh, and Vincent Vanhoucke. Google scanned objects: A high-quality dataset of 3d scanned household items. In *2022 International Conference on Robotics and Automation (ICRA)*, pages 2553–2560. IEEE, 2022.
- [19] Sudharshan Suresh, Zilin Si, Stuart Anderson, Michael Kaess, and Mustafa Mukadam. Midastouch: Monte-carlo inference over distributions across sliding touch. In *Conference on Robot Learning*, pages 319–331. PMLR, 2023.
- [20] Tomáš Hodaň, Martin Sundermeyer, Bertram Drost, Yann Labbé, Eric Brachmann, Frank Michel, Carsten Rother, and Jiří Matas. Bop challenge 2020 on 6d object localization. In *Computer Vision—ECCV 2020 Workshops: Glasgow, UK, August 23–28, 2020, Proceedings, Part II 16*, pages 577–594. Springer, 2020.
- [21] Kaiming He, Georgia Gkioxari, Piotr Dollár, and Ross Girshick. Mask r-cnn. In *Proceedings of the IEEE international conference on computer vision*, pages 2961–2969, 2017.
- [22] Y. Labbe, J. Carpentier, M. Aubry, and J. Sivic. Cosypose: Consistent multi-view multi-object 6d pose estimation. In *Proceedings of the European Conference on Computer Vision (ECCV)*, 2020.
- [23] Yongzhi Su, Mahdi Saleh, Torben Fetzer, Jason Rambach, Nassir Navab, Benjamin Busam, Didier Stricker, and Federico Tombari. ZebraPose: Coarse to fine surface encoding for 6dof object pose estimation. In *Proceedings of the IEEE/CVF Conference on Computer Vision and Pattern Recognition*, pages 6738–6748, 2022.
- [24] Sergey Zakharov, Ivan Shugurov, and Slobodan Ilic. Dpod: 6d pose object detector and refiner. In *Proceedings of the IEEE/CVF International Conference on Computer Vision*, pages 1941–1950, 2019.
- [25] Tomas Hodan, Daniel Barath, and Jiri Matas. Epos: Estimating 6d pose of objects with symmetries. In *Proceedings of the IEEE/CVF conference on computer vision and pattern recognition*, pages 11703–11712, 2020.
- [26] Anna Yershova, Swati Jain, Steven M. LaValle, and Julie C. Mitchell. Generating uniform incremental grids on $so(3)$ using the hopf fibration. *The International Journal of Robotics Research*, 29(7):801–812, Nov 2009.
- [27] Norman Mu, Alexander Kirillov, David Wagner, and Saining Xie. Slip: Self-supervision meets language-image pre-training. In *Computer Vision—ECCV 2022: 17th European Conference, Tel Aviv, Israel, October 23–27, 2022, Proceedings, Part XXVI*, pages 529–544. Springer, 2022.
- [28] Alec Radford, Jong Wook Kim, Chris Hallacy, Aditya Ramesh, Gabriel Goh, Sandhini Agarwal, Girish Sastry, Amanda Askell, Pamela Mishkin, Jack Clark, et al. Learning transferable visual models from natural language supervision. In *International conference on machine learning*, pages 8748–8763. PMLR, 2021.
- [29] Hugues Thomas, Charles R Qi, Jean-Emmanuel Deschaud, Beatriz Marcotegui, François Goulette, and Leonidas J Guibas. Kpconv: Flexible and deformable convolution for point clouds. In *Proceedings of the IEEE/CVF international conference on computer vision*, pages 6411–6420, 2019.

A Comparison with only zero-shot pose estimation

Since the current zero-shot pose estimation method, Megapose [5], operates within the supervised instance segmentation setting, it is necessary to establish a fair comparison with our proposed zero-shot pose estimator. To achieve this, we integrate the zero-shot instance segmentation results with the segmentation results obtained through supervised training using MaskRCNN [21], which aligns with Megapose’s methodology.

Compared to Megapose, our proposed zero-shot pose estimator exhibits a significant performance gain in terms of the mean average recall (AR) score across the seven BOP core datasets, increasing from 17.7% to 25.0%. Our method generally outperforms Megapose 8.6% in terms of the mean average recall (AR) score. For LM-O and T-LESS datasets, the performance is comparable because there is a limitation from the low signal-to-noise ratio of the scene’s point clouds. The number of points from the scene object region is too small and the percentage of noise from the depth sensor or segmentation result will be increased. Consequently, the accuracy of the scene’s geometric structure is compromised, making it challenging to estimate the correct pose accurately.

Table 7: Evaluation of zero-shot pose estimation results on the BOP dataset. The metric is the Average Recall(AR) in BOP Challenge [20].

Method	ZSIS	ZSPE	LM-O	T-LESS	TUD-L	IC-BIN	ITODD	HB	YCB-V	Mean
MegaPose[5]	✗	✓	18.7	19.7	20.5	15.3	8.00	18.6	13.9	16.4
Ours	✗	✓	15.2	19.2	30.6	25.0	24.5	31.6	28.8	25.0
Ours	✓	✓	14.2	6.3	24.9	18.7	13.6	23.6	22.9	17.7

B Pseudo Code

We present the PyTorch-style pseudocode of the proposed zero-shot pose estimation Algorithm 1.

Algorithm 1 The PyTorch-style pseudo code for proposed zero-shot pose estimation

```
Input:  $I_{RGB}, I_D, Objs$   
Output:  $M_{seg}, Rs, ts$   
  
# Inputs parameters:  
# I_{RGB}, I_D: the scene image from the RGB-D sensors  
# Objs: target objects' 3D Models  
  
# Output parameters:  
# M_{seg}: predict instance segmentation results  
# Rs, ts: the estimated pose parameters  
  
# Segment anything by SAM  
SAM.set(I_{RGB}) # scene image (H, W, 3) encoding  
points_prompt = uniform_points(64) # 64 points per image side  
# foreground instances masks without labels  
Masks = SAM(points_prompt) # (M, H, W)  
  
# Label out candidate masks  
# Crop the image region from the scene image by masks  
candidate_images = crop_resize(I_{RGB}, Masks, 224) # (M, 224, 224, 3)  
#extract visual features by a pretrained ViT model.  
candidate_features = ViT(candidate_images) # (M, C)  
# L2 normalize  
candidate_features = F.normalize(candidate_features, dim=-1)  
# extract the rendered template images.  
# N target objects with R rendered template images per object.  
template_features = ViT(template images) # (N, R, C)  
# L2 normalize  
template_features = F.normalize(template_features, dim=-1)  
# cosine similarity  
logits = torch.einsum('mc,nrc->mnr', [candidate_features, template_features])  
# adopt the max similarity from different templates for each object  
logits = logits.max(-1).values # (M, N)  
valid_mask, valid_cls = torch.where(logits > thres)  
# Select the max similarity object as the label for each candidate masks  
masks, object_ids = index_mask_with_logits(valid_mask, valid_cls, logits)  
M_{seg} = zip(masks, object_ids)  
  
# zero-shot pose estimation  
# xyz = project(I_D, K) # project depth to XYZ of camera intrinsic para K.  
# sample point could from target objects' 3D models  
obj_pcs = uniform_sample(Objs)  
obj_radius = radius(obj_pcs) # calculate the radius of objects  
Rs, ts = [], []  
for mask, oid in zip(masks, object_ids):  
    # obj point clouds as src point  
    src = obj_pcs[oid] # (P, 3)  
    # scene object point cloud as ref point  
    ref = xyz[mask] # (Q, 3)  
    # Filter the noisy points by object radius  
    o_r = obj_radius[oid]  
    ref_clean = filter(ref, o_r)  
    # Estimate the pose transformation from src to ref  
    R, t = point_matching(src, ref)  
    Rs.append(R)  
    ts.append(t)  
  
return M_{seg}, Rs, ts
```
